



COPY RIGHT

2017 IJIEMR. Personal use of this material is permitted. Permission from IJIEMR must be obtained for all other uses, in any current or future media, including reprinting/republishing this material for advertising or promotional purposes, creating new collective works, for resale or redistribution to servers or lists, or reuse of any copyrighted component of this work in other works. No Reprint should be done to this paper, all copy right is authenticated to Paper Authors

IJIEMR Transactions, online available on 16th Aug 2017. Link

[:http://www.ijiemr.org/downloads.php?vol=Volume-6&issue=ISSUE-7](http://www.ijiemr.org/downloads.php?vol=Volume-6&issue=ISSUE-7)

Title: **A NOVEL METHOD FOR IMPROVING BORESIGHT RADIATION BANDWIDTH BY METAMATERIAL INLEAKY-WAVEANTENNA**

Volume 06, Issue 07, Pages: 156 – 164.

Paper Authors

GANGAIAH KAYAKOKULA,SK.MUNWAR ALI

Eswar College Of Engg ,Narasaraopet



USE THIS BARCODE TO ACCESS YOUR ONLINE PAPER

A NOVEL METHOD FOR IMPROVING BORESIGHT RADIATION BANDWIDTH BY METAMATERIAL INLEAKY-WAVEANTENNA

¹ GANGAIAH KAYAKOKULA, ² SK.MUNWAR ALI

¹PG Student Dept Of E.C.E Eswar College Of Engg ,Narasaraopet

²Asst professor, Dept Of E.C.E Eswar College Of Engg ,Narasaraopet

Abstract— Improvement of boresight radiation Bandwidth in leakywave antenna is a primary concern. The novelty of our proposed method is based on using substrate integrated metamaterial. The proposed leaky-wave antenna based on a composite right/left-handed substrate integrated waveguide consists of two leaky-wave radiator elements which are with different unit cells. The dual-element antenna prototype features boresight gain of 12.0 dBi with variation of 1.0 dB over the frequency range of 8.775-9.15 GHz or 4.2%. In addition, the antenna is able to offer a beam scanning from -60° to 60° with frequency from 8.25 GHz to 13.0 GHz.

Keywords— Beam scanning, leaky-wave antenna, metamaterial, substrate integrated waveguide, wideband boresight radiation.

I. INTRODUCTION

Leaky-wave antennas (LWAs) have been received much attention in recent years for applications in the microwave and millimeter-wave systems. Planar LWAs [1] have been used in many applications because of the attractive properties such as low profile, beam scanning, and easy integration with other planar components. An LWA is able to achieve backward and boresight radiations using metamaterials such as the composite right/left-handed (CRLH) structures [2]. The CRLH transmission-line based LWAs can improve boresight gain over a narrow frequency band when a balanced condition (when series resonance equal to shunt resonance) is satisfied. If a CRLH structure is unbalanced, a stop-band gap region is generated between the left-handed region and the right-handed region. The stop-band gap region is undesirable for

the antenna applications because it prevents the boresight radiation and thus degrades the boresight gain at the transition frequency. A number of metamaterial-based LWAs have been reported in the literature for achieving continuous radiation from the backward to forward direction. However, the boresight radiation of these antennas suffers very narrow bandwidth, when compared with the radiation in the left-handed and right-handed regions [2-7]. An antenna with 25 unit cells was positioned on a concave surface to get uniform radiation beams reported in Refs. [8] and [9]. An LWA comprising two CRLH transmission-line structures was presented to steer its main beam around 10.0 GHz using the port excitations (four ports) [10]. The conventional CRLH based LWAs discussed above are with the narrow bandwidth for boresight radiation. The LWAs for the

boresight radiation have also been proposed based on different aperture-shaped structures [11-21]. Recently, a surface wave holographic antenna excited by a traveling wave patch array was proposed [11] to improve the bandwidth of boresight radiation. An analysis of the radiation characteristics of the CRLH LWAs around boresight was discussed in Ref. [12]. The boresight gain can be significantly improved by periodically perturbing the spacing of the hole lattice based LWA [13]. In [20], a radial LWAs array was reported to achieve boresight radiation, where the eight SIW LWAs array was fed at the centre by a vertically polarized point source. In this paper, a substrate integrated CRLH-based LWA is proposed for wideband boresight radiation. The proposed LWA consists of two slotted elements that are composed with 15 slot/patch cells, respectively. The size of the cells is optimized to achieve the wideband boresight radiation. The design procedures are also provided. The antenna was fabricated and measured. The simulations are carried out by CST Microwave Studio [22].

II. ANTENNA CONFIGURATION AND DESIGN

The structure of the proposed LWA is shown in Fig. 1. The input and output of the slanted- and vertical-slotted LWA elements are connected to the power dividers at the both ends of the structure. The dual-element configuration is proposed to improve the boresight radiation of the antenna. Each CRLH based element is designed using a multilayered substrate integrated waveguide (SIW) structure consisting of an embedded

patch array and a slot array. The dielectric substrate

Is RT/Duroid 5880 with $\epsilon_r = 2.2$ and $\tan\delta = 0.0009$.

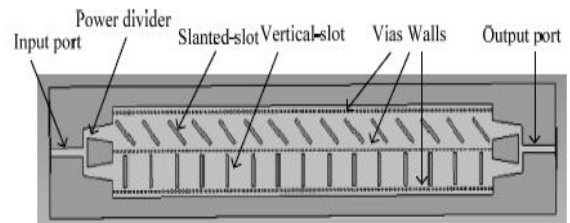
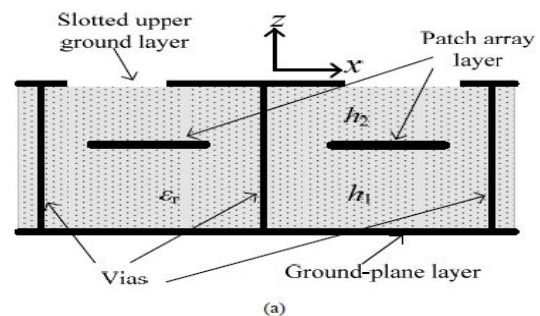


Fig. 1. Proposed CRLH-based dual-element LWA.

Fig. 2(a) shows the cross-sectional view and the unit cell of the proposed CRLH LWA. The unit cell of the dual-element LWA is shown in Fig. 2(b). It consists of dual embedded patches with dual slots cut onto the upper layer. Note that the embedded patches are right underneath the slots. The slots with the embedded patches are used to generate the series capacitance, while the shunt inductance can be generated by vias walls for the left-handed metamaterials [4]. One slot is slanted at 45° to widen the bandwidth of boresight radiation. The slotted upper ground plane and the lower ground plane are connected through metallic via walls. The vertical-slotted and slanted-slotted SIW leaky-wave radiator elements are combined using a common via wall



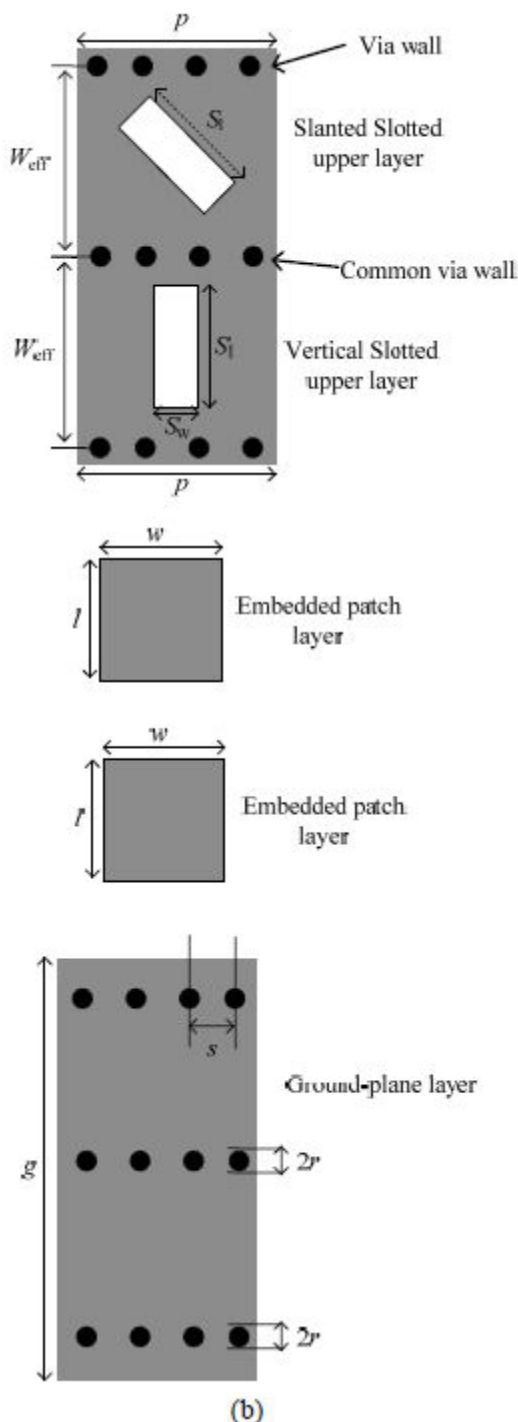


Fig. 2. The proposed dual elements based LWA: (a) cross-sectional view and (b) unit cell.

The design procedures of the antenna are summarized as below;

a) Design the dual CRLH based unit cells (one with vertical rectangular slot and the other with slanted rectangular slot) with a balanced condition of $\beta = 0$ at the center operating frequency (The boresight radiation occurs at the frequency when balanced condition occurs). The balanced condition is dependent on the size of embedded patch and slot.

b) Choose the number of the dual unit cells based on the gain requirements. Generally, the LWA with more unit cells features higher gain. However, there is a limitation for the gain enhancement with the increasing of the unit cells [23].

c) If desired gain at the boresight is not achieved, increasing the number of the slot element or modifying slightly the embedded patch size and slanted slot length is suggested.

As an example, the unit cell of the proposed LWA is designed with transition frequency or balanced condition at around 9.0 GHz. The details of the unit cell of the structure are shown in Fig. 2(b). The optimized dimensions for the balanced condition at around 9.0 GHz are: $p = 10.2$ mm, ground-plane layer width, $g = 40$ mm, metallic via diameter, $2r = 0.76$ mm, spacing from via center to via center, $s = 1.52$ mm, embedded patch area, $l \times w = 4.9$ mm \times 3.925 mm, $W_{eff} = 11.8$ mm, upper-layer slot width, $S_w = 1.0$ mm, slanted-slot length, $S_l = 9.45$ mm, and vertical-slot length, $S_l = 9.35$ mm. The dual embedded patches are positioned at the substrate height of $h_1 = 0.66$ mm. The overall height is $h_1 + h_2 = 0.914$ mm.

The dispersion diagram (phase constant with frequency) of the unit cell is studied using the commercial CST software, Eigen mode solver [22] and plotted in Fig. 3. In parameter sweep, the phase was varied from 0 to 180 degrees. The mesh type was selected tetrahedral mesh and modes of 2. The balanced condition of $\beta = 0$ is achieved around 9.0 GHz. The air-line $(k_o = \omega \sqrt{\epsilon_o \mu_o})$ crosses the right-handed upper frequency around 13.25 GHz and left-handed lower frequency around 8.25 GHz. The left-handed region ranges from 8.25 to 9.0 GHz and the right-handed region from 9.0 to 13.25 GHz. The gain with respect to the number of the proposed dual-unit cell is shown in Fig. 4.

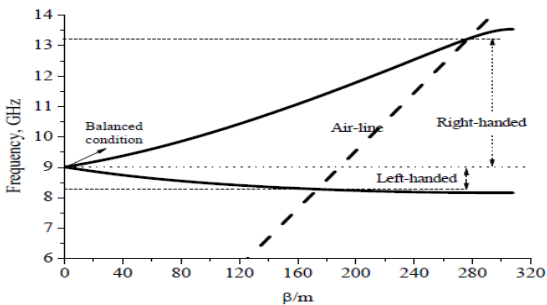


Fig. 3. Dispersion diagram of the unit cell.

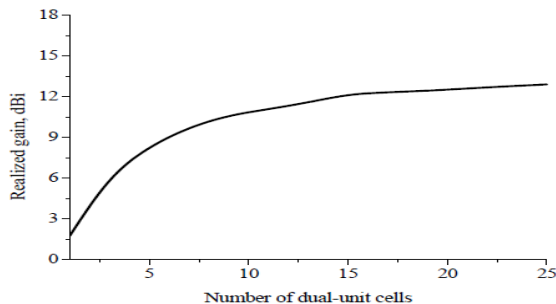


Fig. 4. Realized boresight gain with number of dual-unit cells at 9.0 GHz.

III. RESULTS AND DISCUSSIONS

The LWAs with single vertical- or slanted-slot radiator were also designed for

comparison. The simulated realized gains at the boresight of the antennas are compared. All three antennas were designed with 15 unit cells and optimized for the bore sight radiation (along z-axis). Fig. 5 exhibits the realized gain of the antennas at the boresight. The proposed LWA shows the wider boresight 1-dB gain bandwidth of 375 MHz over the 175 MHz of the single vertical- or slanted-slotted LWA. The vertical- and slanted-slotted LWAs are with almost same 1-dB gain bandwidth at the boresight. The enhancement of the boresight gain bandwidth is attributed to the combination of the radiation from the slanted-slotted and the vertical-slotted elements. The cross-polarization of the proposed antenna is also exhibited in the Fig. 5, which is around 10 dB. The realized gain at boresight and cross-polarization with combination of vertical slot (0°) and angle variation of slanted slot (45°) are compared in Fig. 6. A combination of 0° and 45° slots shows the wider 1-dB gain bandwidth at the boresight.

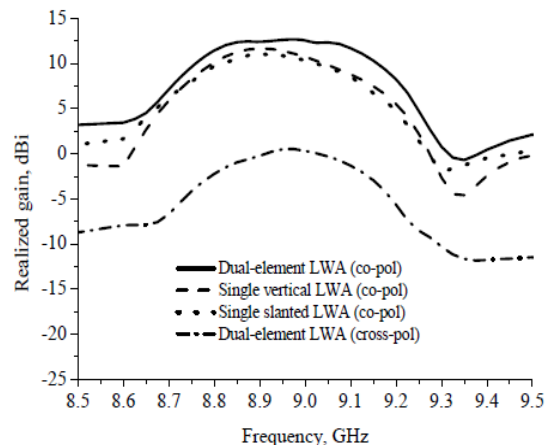


Fig. 5. Realized boresight gain of the single vertical-, slanted-slotted, and proposed dual-element LWAs.

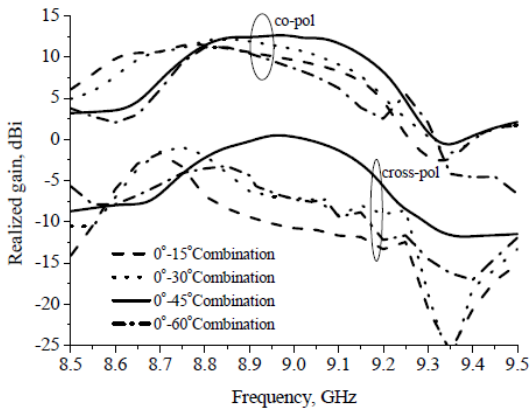


Fig. 6. Realized gain and cross-polarization with angle variation of slanted slot.

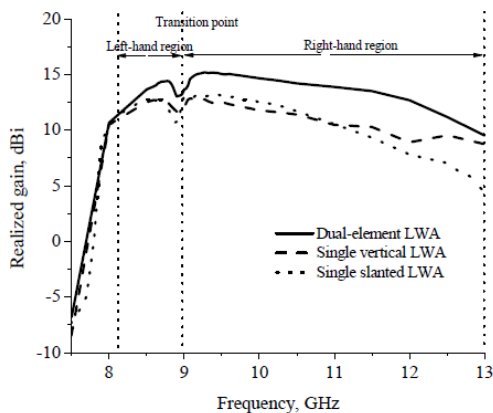


Fig. 7. Maximum realized gain of the antennas.

The maximum realized gains of the antennas are shown in Fig. 7. The proposed dual-element LWA shows a higher gain over the frequency band with antenna efficiency more than 75%. The single slanted- and vertical-slotted LWAs show almost same gain up to 12 GHz. The proposed antenna was fabricated and measured. Fig. 8 illustrates the photo of the antenna prototype as well as the dimensions (in mm) of feeding network. The overall size of the antenna is 200 mm x 40 mm x 0.914 mm. The antenna is excited at the left end and 50-Ω loaded at the right end for radiation parameters measurement. Fig. 9 shows the comparison

of the simulated and measured $|S_{11}|$ and $|S_{21}|$ of the antenna prototype. The transition point (balanced condition point) of the left-handed and the righthand regions occurs at around 9.0 GHz. The frequency range of the left-handed region is from 8.25 to 9.0 GHz and the right-handed region from 9.0 to 13.25 GHz. The left-handed region is narrower than the right-handed region. The ripples on the $|S_{21}|$ curve come from the coupling between the vertical-slotted and the slanted-slotted elements. Note that the slanted-slotted element has strong coupling with the vertical slotted element, there is no any ripples on the $|S_{21}|$ when both elements are with vertical-slotted. The simulated results follow the measured results for S-parameters.



Fig. 8. Photo of the dual elements based LWA antenna prototype.

The measured and simulated gain of the antenna prototype at the boresight is compared in Fig. 10. The measured 1-dB gain bandwidth is around 375 MHz (8.775-9.15 GHz). The measured maximum boresight gain is 13.1 dBi at 9.0 GHz. A good agreement is achieved between the simulated and the measured gain at the boresight.

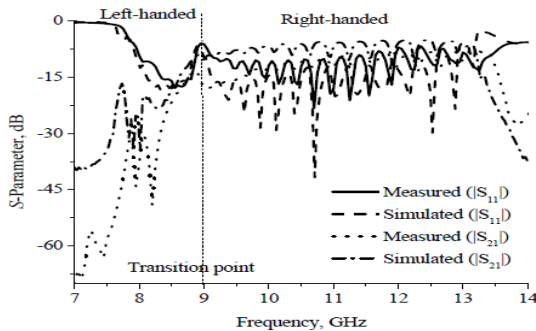


Fig. 9. Measured and simulated S -parameters ($|S_{11}|$ and $|S_{21}|$).

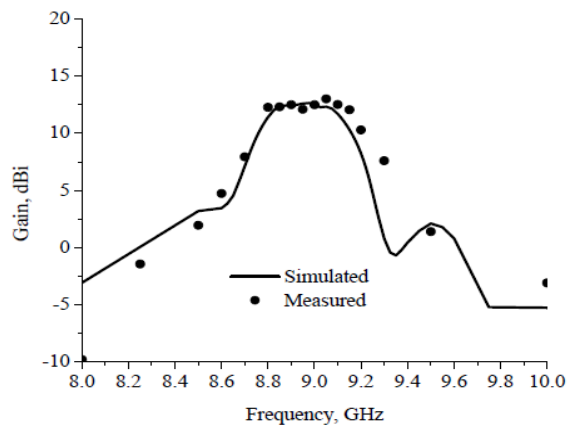


Fig. 10. Measured and simulated gains at the boresight.

The simulated and measured maximum gains are exhibited in Fig. 11, wherein a good agreement is achieved as well. At the transition point, the gain is slightly lower. The maximum measured gain is around 14.8 dBi at 9.5 GHz. A small gain dip is at 9.0 GHz in the transition region. The beam scanning angle and 3-dB beamwidth are measured and compared with simulations in Fig. 12, where good agreement is observed. The measured beam scanning angle is from -60 to 66 over the frequency range from 8.25 to 13.25 GHz. At around 9.0 GHz, the wideband boresight radiation is achieved. The measured 3-dB beamwidth (around 10 degrees) is consistent over the frequency band of 8.5-13.0GHz.

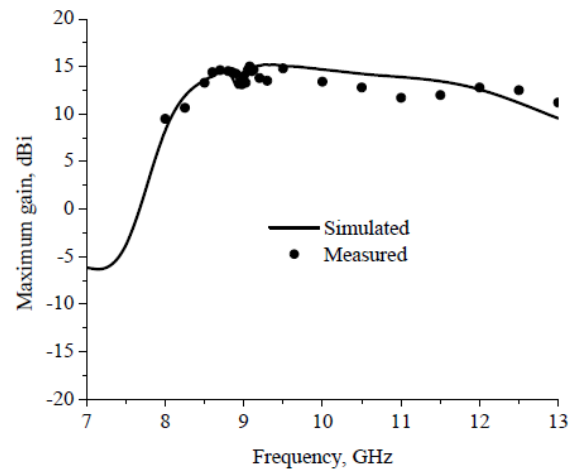


Fig. 11. Maximum measured and simulated gains.

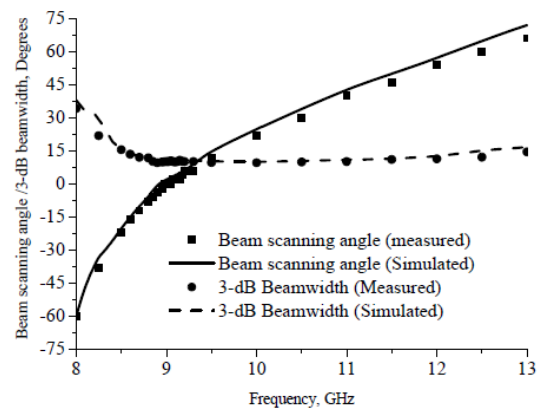
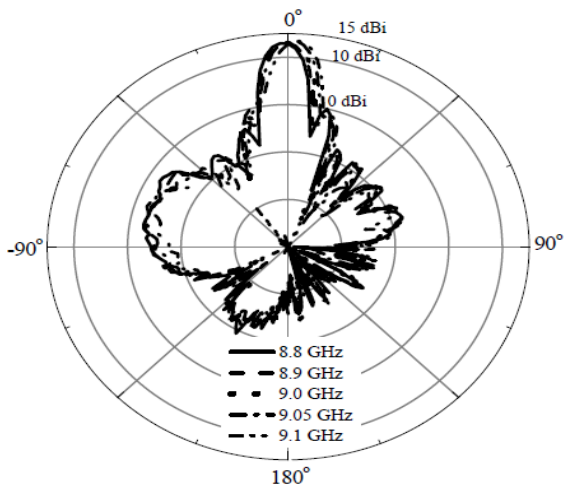
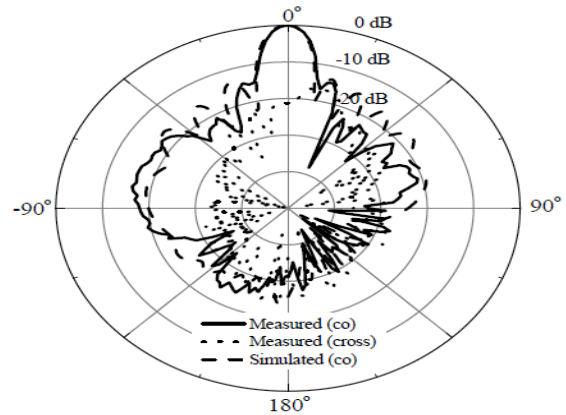


Fig. 12. Measured and simulated beam scanning angle and 3-dB beamwidth.

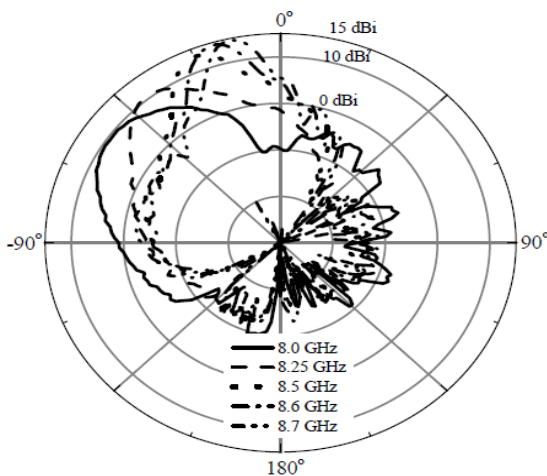
The measured radiation patterns around the transition point of 8.8, 8.9, 9.0, 9.05, and 9.1 GHz are plotted in Fig. 13(a). At all these frequencies, the main beam is directed to the boresight and the 3-dB beamwidth is also consistent (around 10 degrees). The radiation patterns at the frequencies are almost the same. The front to back ratio is better than 25 dB for the left-handed (8.0, 8.25, 8.5, 8.6, and 8.7 GHz) and right-handed (9.5, 10.0, 10.5, 11.5, and 12.5 GHz) regions, the measured radiation patterns are plotted in Figs. 13(b) and 13(c), respectively.



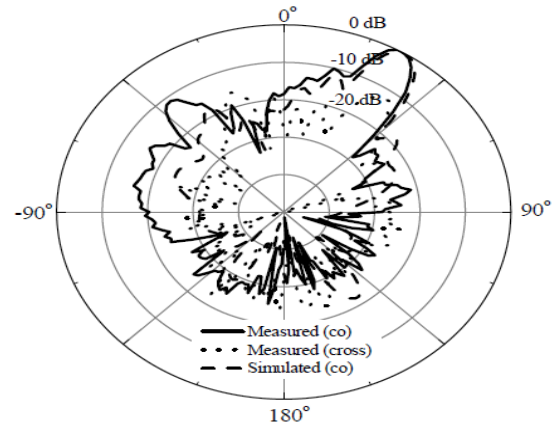
(a)



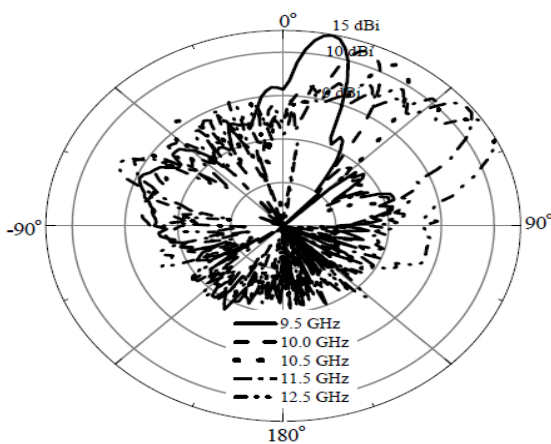
(b)



(b)



(c)



(c)

Fig. 13. Measured radiation patterns of the antenna: (a) at around balanced condition, (b) left-handed region, and (c) right-handed region.

Fig. 14. Measured and simulated normalized radiation patterns: (a) left-handed region ($f = 8.25$ GHz), (b) balanced condition ($f = 9.0$ GHz), and (c) right-handed region ($f = 10.5$ GHz).

Figs. 14(a)-(c) compares the measured and simulated radiation patterns at 8.25, 9.0, and 10.5 GHz, which correspond to the radiation from the left-handed, transition, and right-handed regions, respectively. At 8.25 GHz, the beam is backward directed, while the beam is along the forward direction at 10.5 GHz. The measured and simulated radiation patterns are in good agreement in all three regions. The 3-dB beamwidth (22 degrees) at 8.25 GHz is larger compared to those (10 degrees) at 9.0 GHz and 10.5 GHz. The side-lobes are less than -10 dB for all

frequency points within the band of 8.25-13.0 GHz. The measured cross-polarization patterns at 8.25, 9.0, and 10.5 GHz are also demonstrated, the cross polarization level is lower than 12 dB in all regions.

IV. CONCLUSION

A substrate integrated leaky-wave antenna has been proposed to double the bandwidth of the boresight radiation based on a dual-element structure. The proposed LWA has achieved a wideband consistent boresight radiation and a continuous scanning radiation with an angle of $\pm 60^\circ$. Some design guidelines have been also described for antenna designers. The proposed structure is useful for wideband boresight radiation of the LWA with high gain.

REFERENCES

- [1] Y. Qian, Y. Qian, B.C.C. Chang, T. Itoh, K. C. Chen, and C. K. C. Tzuang, "High efficiency and broadband excitation of leaky mode in microstrip structures," *International Microwave Symposium Digest, MTT-S*, vol. 4, pp. 1419–1422, 1999.
- [2] C. Caloz and T. Itoh, *Electromagnetic Metamaterials: Transmission line theory and microwave applications*, New York, John Wiley & Sons, 2004.
- [3] L. Liu, C. Caloz, and T. Itoh, "Dominant mode (DM) leaky-wave antenna with backfire-to-endfire scanning capability," *Electronics Letters*, vol. 38, no. 23, pp. 1414–1416, Nov. 2002.
- [4] Y. D. Dong and T. Itoh, "Composite right/left-handed substrate integrated waveguide and half mode substrate integrated waveguide leaky-wave structures," *IEEE Trans. Antennas and Propagation*, vol. 59, no. 3, pp. 767–775, Mar. 2011.
- [5] Y. D. Dong and T. Itoh, "Composite right/left-handed substrate integrated waveguide leaky-wave antennas," *Proceeding of 39th European Microwave Conference*, pp. 276–279, 2009.
- [6] Y. Weitsch and T. F. Eibert, "Analysis and design of a composite left/right-handed leaky wave antenna based on the H10 rectangular waveguide mode," *Advances in Radio Science*, 6, 49–54, 2008.
- [7] Y. Mizumori, K. Kubo, M. Kishihara, J. Yamakita, and I. Ohta, "Backfire-to-endfire radiation characteristics of CRLH-TL using substrate integrated waveguide and metal-patches," *Asia-Pacific Microwave Conference*, pp. 1419–1422, 2009.
- [8] M. R. M. Hashemi and T. Itoh, "Dispersion engineered metamaterial based transmission line for conformal surface application," *International Microwave Symposium Digest, MTT-S*, pp. 331–334, 2008.
- [9] M.R.M. Hashemi and T. Itoh, "Composite right/left-handed leaky-wave antenna for concave surfaces," *IEEE International Workshop on Antenna Technology (iWAT 2009)*, 2009.
- [10] M. A. Eberspacher and T.F. Eibert, "Leaky wave antenna with amplitude controlled beam steering based on composite right/left-handed transmission lines," *Advances in radio Science*, 8, pp. 27–32, 2010.

- [11] A. Sutinjo and M. Okoniewski, "A surface wave holographic antenna for broadside radiation excited by a traveling wave patch array," *IEEE Trans. Antennas and Propagation*, vol. 59, no. 1, pp. 297–300, Jan. 2011.
- [12] J. S. Gomez-Diaz, A. Alvarez-Melcon, and J. Perruisseau-Carrier, "Analysis of the radiation characteristics of CRLH LWAs around broadside," 6th *European Conference on Antennas and Propagation (EUCAP)*, 2012, pp. 2876–2880, 2012.
- [13] N. Gagnon, A. Ittipiboon, and A. Petosa, "Design of a leaky-wave antenna for broadside radiation," *IEEE Antennas and Propagation Society International Symposium*, 2006, pp. 361 – 364, 2006.
- [14] G-F. Cheng and C-K. C. Tzuang, "Small planar broadside radiation leaky wave antenna design," *IEEE Antennas and Propagation Society International Symposium*, 2010, pp. 1 – 4, 2010.
- [15] S. K. Podilchak, A. P. Freundorfer, and Y. M. M. Antar, "Segmented circular strip planar leaky-wave antenna designs for broadside radiation and one-sided beam scanning," *IEEE International Workshop on Antenna Technology (iWAT 2010)*, pp. 1 – 4, 2010.
- [16] S. K. Podilchak, A. P. Freundorfer, and Y. M. M. Antar, "Planar leakywave antenna designs offering conical-sector beam scanning and broadside radiation using surface-wave launchers," *IEEE Antennas and Wireless Propagation Letters*, vol. 7, pp. 155 – 158, 2008.
- [17] N. Gagnon, A. Petosa, and A. Ittipiboon, "Design of a strip-line leaky wave antenna for broadside radiation," *European Conference on Antennas and Propagation (EUCAP)*, 2012, pp. 1–7, 2012.
- [18] G. Lovat, P. Burghignoli, and D. R. Jackson, "Fundamental properties and optimization of broadside radiation from uniform leaky-wave antennas," *IEEE Trans. Antennas and Propagation*, vol. 54, no. 5, pp. 1442–1452, May 2006.
- [19] S. Paulotto, P. Burghignoli, F. Frezza, and D. R. Jackson, "Full-wave modal dispersion analysis and broadside optimization for a class of microstrip CRLH leaky-wave antennas," *IEEE Trans. Antennas and Propagation*, vol. 56, no. 12, pp. 2826–2837, Dec. 2008.
- [20] A. J. Martinez-Ros, J. L. Gomez-Tornero, and G. Goussetis, "Broadside radiation from radial arrays of substrate integrated leaky-wave antennas," 6th *European Conference on Antennas and Propagation (EUCAP)*, 2012, pp. 252–254, 2012.
- [21] T. R. Cameron, A. T. Sutinjo, and M. Okoniewski, "A circularly polarized broadside radiating "Herringbone" array design with the leaky-wave approach," *IEEE Antennas and Wireless Propagation Letters*, vol. 9, pp. 826–829, 2010.
- [22] CST Microwave Studio, version 2011.06, 2012.
- [23] Nasimuddin, Z. N. Chen, and X. Qing, "Multilayered composite right/left-handed leaky-wave antenna with consistent gain," *IEEE Trans. Antennas and Propagation*, vol. 60, no. 11, pp. 5056–5062, Nov. 2012.